Springer

KSME

Journal of Mechanical Science and Technology 29 (1) (2015) 5~10
www.springerlink.com/content/1738-494x
DOI 10.1007/s12206-014-1201-4

Fracture property of double cantilever beam of aluminum foam bonded with spray adhesive †

Moon Sik Han[1], Hae Kyu Choi[2], Jae Ung Cho[2,*] and Chong Du Cho[3]

[1]*Department of Mechanical and Automotive Engineering, Keimyung University, 2800 Dalgubeoldaero, Dalseo-Gu, Daegu, 704-701, Korea,*
[2]*Division of Mechanical and Automotive Engineering, Kongju National University, 1223-24 Cheonan Daero, Seobuk-gu, Cheonan-si, Chungnam, 331-717, Korea*
[3]*Department of Mechanical Engineering, Inha University, 253, Yonghyeon-dong, Nam-gu, Incheon, 402-751, Korea*

(Manuscript Received April 30, 2014; Revised April 30, 2014; Accepted May 7, 2014)

Abstract

Aluminum foam with the property of excellent impact absorption has been widely used recently. It is necessary to study fracture energy due to energy release rate by the use of adhesive joint at aluminum foam. This study aims at strength evaluation about adhesive joint on aluminum foam. Bonded DCB specimens with this material property are experimented and the fracture behavior is analyzed by simulation. These specimens are designed by differing in height on the basis of British industrial and ISO standards. As the value of height at model is higher, bonded part is separated to the end. By comparing analysis results with experimental data, these data could agree with each other. By the confirmation with experimental results, these all simulation results in this study can be applied on real composite structure with aluminum foam material effectively. The fracture behavior and its property can also be examined by this study.

Keywords: Aluminum foam; Double cantilever beam; Fracture energy; Fracture property

1. Introduction

The study on aluminum foam has been focusing on manufacturing method, sound absorption, and shock absorption. The study on aluminum foam adhesion, however, has been far behind despite its importance. To ensure the safe application of the coupling method for adhesion structure, the data on fracture toughness is important. Currently on strength evaluation, the method using fracture mechanics has been progressively adopted. As the part of evaluation method using fracture mechanics, double cantilever beam (DCB) specimen when cracks are developed (mode I) at the only open mode has been often used to understand the fracture behavior of adhesion surface, including delamination, as well as to measure fracture toughness. Such approach has been modified as standard specification over an extended period [1-5]. DCB specimen of aluminum foam composite material [6-8] is fabricated and the test at mode I is carried out according to British standard [9] and ISO [10]. As finite element method is carried with modeling the same configuration as experimental specimen, these analysis results are compared with experimental results. The broken shape of the bonded specimen with aluminum foam applied by static load is investigated. This study result is thought to suggest the basic data necessary at durable safe design.

*Corresponding author. Tel.: +82 41 521 9271, Fax.: +82 555 9123
E-mail address: jucho@kongju.ac.kr
† This paper was presented at the FEOFS 2013, Jeju, Korea, June 9-13, 2013.
Recommended by Guest Editor Jung-Il Song

2. Experiment and analysis

2.1 Theory background

2.1.1 Critical energy release rate (G_{IC})

In mode I condition, G_{IC} or critical fracture energy is calculated by using Eq. (1) [9]:

$$G_{IC} = \frac{P^2}{2B}\frac{dC}{da} \tag{1}$$

where C is the compliance by δ/P, B is the width of the specimen, P is the load measured by load cell of the tester and a is the length of the crack. C is calculated from bending and shear deformation and obtained from relational expression such as Eq. (2).

$$\frac{dC}{d_a} = \frac{8}{E_S B}\left(\frac{3a^2}{h^3} + \frac{1}{h}\right) \tag{2}$$

where E_S is elastic modulus of the beam and h is the height of the beam. By differentiating Eq. (2) and substituting to Eq. (1),

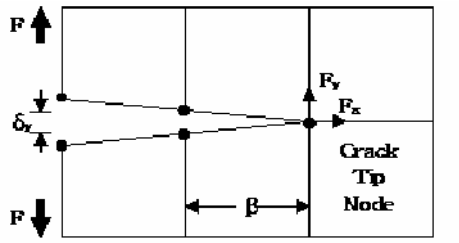

Fig. 1. Nodal force at crack tip.

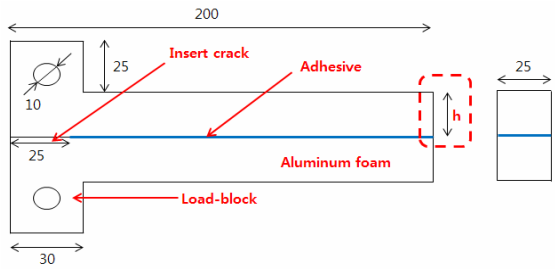

Fig. 2. Dimension of the specimen.

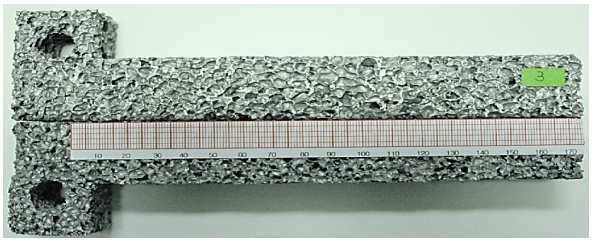

Fig. 3. Photo of fabricated specimen.

the critical fracture energy on simple beam theory is as following Eq. (3).

$$G_{IC} = \frac{4P^2}{E_s B^2}\left(\frac{3a^2}{h^3} + \frac{1}{h}\right) = \frac{4P^2}{E_S B^2} \cdot m \,. \tag{3}$$

However, according to simple beam theory, compliance value is calculated less than actual value because of the assumption that the beam is fastened incompletely. Thus, compliance value C which is closer to the actual value is calculated based on assumption that the beam is fastened completely by using corrected beam theory. A cube root equation of $C^{1/3}$ or $(C/N)^{1/3}$ is drawn and $|\Delta|$ or an intercept value on X-axis is obtained. This value is then included with crack length and expressed as (α +$|\Delta|$). Calculation of critical fracture energy, G_{IC} at mode I load condition is dependent on load condition. In this study, G_{IC} is calculated using Eq. (4) and load block.

$$G_{IC} = \frac{3P\delta}{2B(a+|\Delta|)}\frac{F}{N} \tag{4}$$

where δ is the displacement on load line and Δ is the correction to crack length at the beam which is incompletely fastened. N is corrected value of stiffness by the rotation of the load block and F is the correction factor corresponding to the reduction of bending moment by large deformation. F and N are calculated by Eqs. (5) and (6).

$$F = 1 - \frac{3}{10}\left(\frac{\delta}{a}\right)^2 - \frac{3}{2}\left(\frac{l_1\delta}{a^2}\right) \tag{5}$$

$$N = 1 - \left(\frac{l_2}{a}\right)^3 - \frac{9}{8}\left[1 - \left(\frac{l_2}{a}\right)^2\right]\frac{l_1\delta}{a^2} - \frac{9}{35}\left(\frac{\delta}{a}\right)^2 . \tag{6}$$

Here, l_1 is the vertical distance between the center of load pin and the beam center where the load block is combined. l_2 is the distance between the load pin center and block edge [9].

2.1.2 Energy release rate at analysis (G_{IC})

Total strain energy release rate, G is obtained by use of the nodal force at crack tip and the displacement of next node on the face of crack mouth as shown in Fig. 1. β is the width of crack tip and Fx, Fy, δx and δy are the nodal forces and displacements at X and Y directions respectively.

The load (P) applied to this model increases and the critical energy release rate (Gc) at the crack tip was obtained by the formula at this simulation as Eq. (7) [11].

$$Gc = (Fx\delta x + Fy\delta y)/(2\,\beta) \,. \tag{7}$$

2.2 Specimen and experimental method

DCB specimen is designed and fabricated in accordance with British standard [9] and ISO standards [10]. The adhesive applied at the specimen is 3M's spray 77. Fig. 2 shows the dimension of specimen and the unit of dimension is mm. Four specimens with the height (h) of 25 mm to 40 mm at 5 mm intervals are fabricated to specimen heights of 25, 30, 35, and 40 mm and classified by Case 1~4, respectively. The length of specimen is 200 mm and the width is 25 mm. Load block is designed with the length of 30 mm and the height of 25 mm and hole with the diameter of 10 mm in load-block. Initial crack with the length of 25 mm is set up [12].

The adhesive agent used at manufacturing specimen has the adhesive strength of 0.4MPa as spray type. Its major components are added to isohexane, cyclohexane and SBR Latex Polymer. Fig. 3 shows the photo of specimen. The tape indicating the number of grids shown by crack length is attached on the specimen. To obtain more accurate test data, a number of aluminum foam specimens by case are fabricated by FOAMTECH Co. at Korea and mean values of fatigue experiment results are calculated and evaluated. The property of aluminum foam is also shown by Table 1.

Table 1. Property of aluminum foam.

Property	Value
Young's modulus (GPa)	2.374
Poisson's ratio	0.29
Density (kg/m^3)	400
Yield strength (MPa)	1.8
Shear strength (MPa)	0.29

Table 2. Material properties.

Property	Value
Young's modulus (GPa)	2.374
Poisson's ratio	0.29
Density (kg/m^3)	400
Yield strength (MPa)	1.8
Shear strength (MPa)	0.92

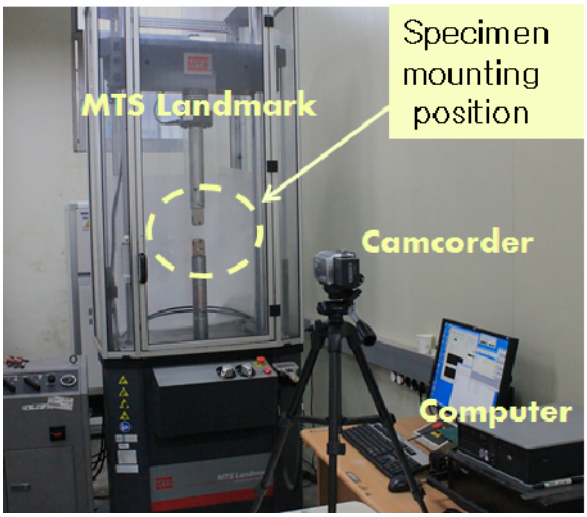

Fig. 4. Installation of test equipment.

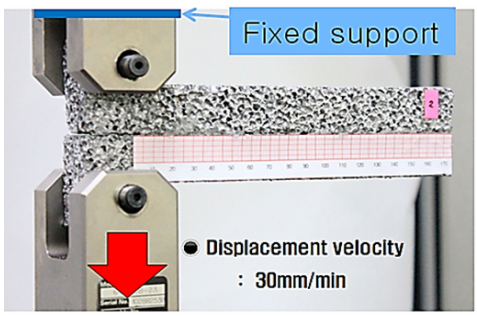

Fig. 5. Experimental setup.

As seen in Fig. 4, MTS' Landmark tester is used for the experiment. These data are produced by using computer and the experimental scenes of each specimen are photographed by using camcorder.

As seen in Fig. 5, the specimen is tied to the jig connected to the load cell and the test is carried out by using displacement control method. Displacement is only vertically imposed on the bottom load cell and the displacement speed is set at 30 mm/min.

2.3 Analysis model and boundary condition

In this study, effective equivalent model is applied because sizes or distributions of pores are not uniform. The analysis result with simplified effective equivalent model can be effectively applied to non-uniform porous foam. Analysis model has the same dimension as experimental specimen. 2 dimensional finite element model of aluminum foam is shown by Fig. 6. This model is divided with rectangular element. The material property is shown by Table 2.

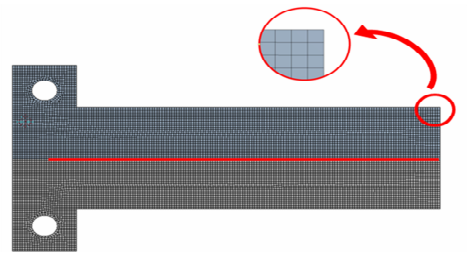

Fig. 6. Finite element model.

As shown by Fig. 6, 2 dimensional finite element model is designed as the same configuration as experimental specimen and is divided with the meshes of rectangular element. The numbers of elements and nodes are 10382 and 32168, respectively. At the part of crack tip, the singularity can be happened. As the density of mesh at this part is enlarged, this effect can be avoided and the stress near crack tip can be calculated. These solution values of reaction forces and energy release rates can be verified by fitting into experimental data.

On the static analysis, bonding force of 4.5 MPa is applied as the limit status just before being separated during experiment. This force is applied perpendicularly on the adhesive face between aluminum foams. If the distance between one and another contact nodes perpendicular to the face becomes 5 mm or more, the two nodes on the face are supposed to be separated each other and the value of adhesive strength is 0. If the distance between one and another contact nodes perpendicular to the face becomes less than 5 mm, the two nodes on the face are supposed to be bonded each other and the value of adhesive strength is 4.5 MPa. This value was measured by finding an average of the data obtained at de-bonding experiment with foam specimen. The damping coefficient is also 10^{-7}. As the same condition as experiment, the pin hole of upper load block is fixed. And the hole of lower load block is applied with the displacement speed of 30 mm/min on the lower direction as shown by Fig. 7. The elapsed time of 40 second is set until thick part is separated.

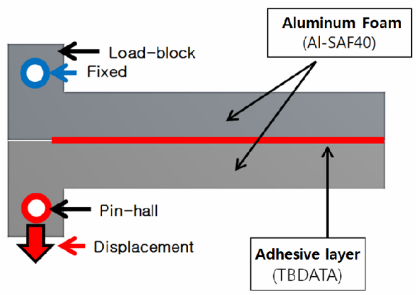

Fig. 7. Boundary condition of analysis.

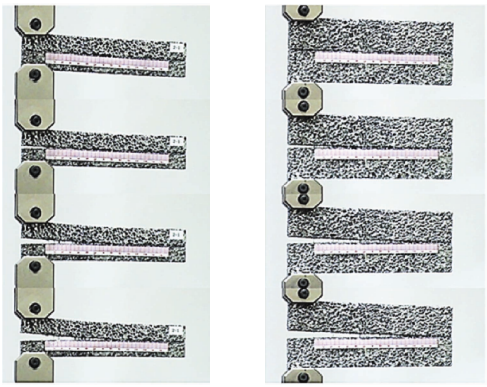

(a) Specimen height 25 mm (b) Specimen height 40 mm

Fig. 8. Segregated specimens during static experiment.

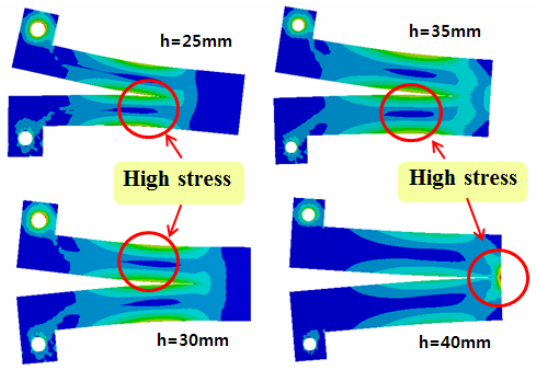

Fig. 9. Contour of equivalent stress at static analysis.

3. Comparison between experiment and analysis result

In cases of specimens with h = 25 and 40 mm, Fig. 8 shows the photos of segregated specimens at an interval of 10 second during static experiment. In case of h = 40 mm, crack is propagated more than the case of h = 25 mm. In case of h = 25 mm, specimen gets bent more than the case of h = 40 mm.

Fig. 9 shows contours of equivalent stress at the elapsed time of 40 seconds in cases of specimen heights of 25, 30, 35 and 40 mm. In cases of specimen heights of 25, 30 and 35 mm, maximum stresses are shown at the end part of crack with the magnitudes of 69, 63 and 54 MPa, respectively. It means that bending force is applied greatly just before the end part of crack in cases of specimen heights of 25, 30 and 35 mm.

In cases of specimen height of 40 mm, maximum stress is shown at the end of bonded part with the magnitudes of 52 MPa. As crack propagates until the rear part of model in case of specimen height of 40 mm, the great stress happens at the rear part of model.

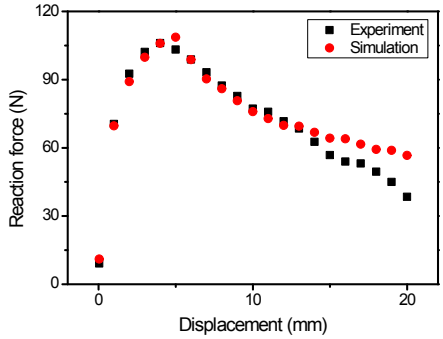

Fig. 10. Graph of reaction force due to displacement (h = 25 mm) in comparison of simulation and experiment.

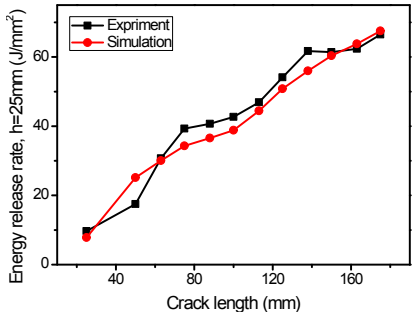

Fig. 11. Graph of energy release rate due to crack length (h = 25 mm) in comparison of simulation and experiment.

Fig. 10 shows reaction force due to the displacement of specimen with h = 25 mm in comparison of simulation and experiment. Experiment and simulation data approach each other. As the displacement of 5 mm, the maximum reaction force shows. And force decreases as displacement increases after this displacement. In case of simulation, reaction force decrease slower than experiment. It means that effective equivalent damage model is applied at simulation but the influence of air is affected between foam material at experiment.

Fig. 11 compares the energy release rate due to crack length in case of specimen with h = 25 mm in comparison of simulation and experiment. The energy release rate increases gradually with the similar slope and maximum energy release becomes 70 J/mm^2 in case of experiment and simulation.

Fig. 12 compares reaction force due to displacement in case of h = 30 mm in comparison of simulation and experiment. Experiment and simulation data approach each other and the maximum reaction force becomes 145 N at displacement of 6 mm. After maximum reaction force, the force decreases rapidly as the displacement increases. In case of simulation, the reaction force decreases slower than experiment. The effective

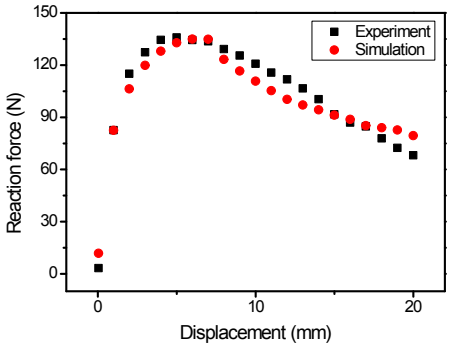

Fig. 12. Graph of reaction force due to displacement (h = 30 mm) in comparison of simulation and experiment.

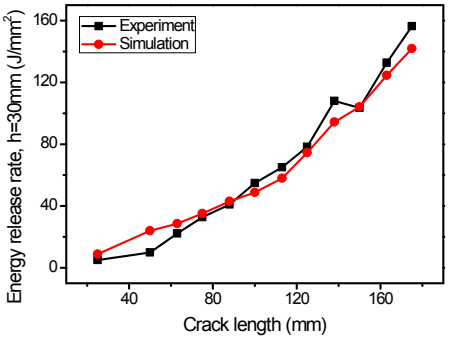

Fig. 13. Graph of energy release rate due to crack length (h = 30 mm) in comparison of simulation and experiment.

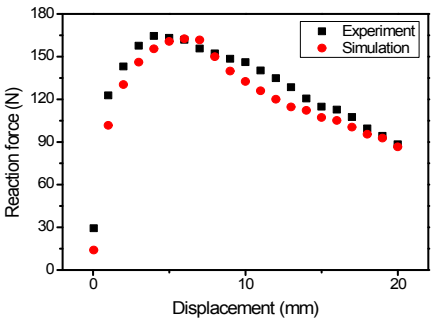

Fig. 14. Graph of reaction force due to displacement (h = 35 mm) in comparison of simulation and experiment.

equivalent damage model is also applied at simulation but the influence of air is affected between foam material at experiment.

Fig. 13 compares energy release rate due to crack length in case of h = 30 mm in comparison of simulation and experiment. The energy release rate increases gradually with the similar slope in case of experiment and simulation. Maximum energy release rate in case of experiment becomes 160 J/mm^2 as much as 15 J/mm^2 a little higher than simulation.

Fig. 14 compares reaction force due to displacement in case of h = 35 mm in comparison of simulation and experiment. Experiment and simulation data approach each other and the maximum reaction force becomes 160 N at displacement of 6 mm. After maximum reaction force, the force decreases as the displacement increases.

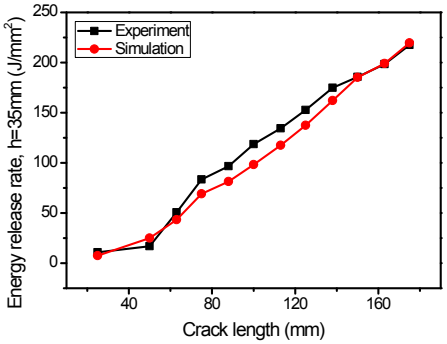

Fig. 15. Graph of energy release rate due to crack length (h = 35 mm) in comparison of simulation and experiment.

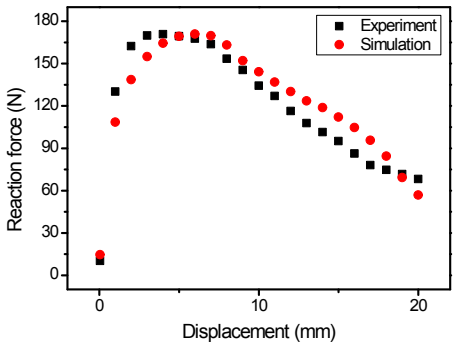

Fig. 16. Graph of reaction force due to displacement (h = 40 mm) in comparison of simulation and experiment.

Fig. 15 compares energy release rate due to crack length in case of h = 35 mm in comparison of simulation and experiment. The energy release rate increases gradually with the similar slope and maximum energy release rate becomes 225 J/mm^2 in case of experiment and simulation.

Fig. 16 compares reaction force due to displacement in case of h = 40 mm in comparison of simulation and experiment. Experiment and simulation data approach each other and the maximum reaction force becomes 170 N at displacement of 5 mm. After maximum reaction force, the force decreases as the displacement increases.

In case of experimental and analysis results, the higher the h, the height of the beam, the greater the maximum load. But the load is significantly reduced as displacement increases.

Fig. 17 compares energy release rate due to crack length in case of h = 40 mm in comparison of simulation and experiment. The energy release rate increases gradually with the similar slope in case of experiment and simulation .

And maximum energy release rate becomes 200 J/mm^2 as displacement increases. After maximum reaction force, the force decreases as the displacement increases. After the length of crack reached 150 mm, G CBT value in case of h = 40 mm is significantly reduced to the level below the data in case of h = 35 mm. It means that specimen is thought to be completely

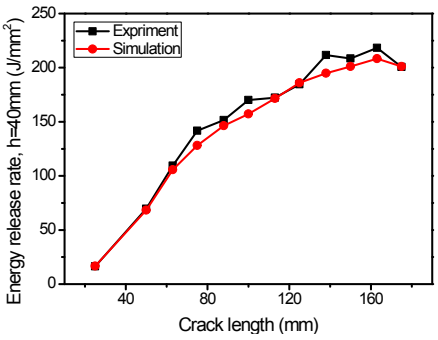

Fig. 17. Graph of energy release rate due to crack length (h = 40 mm) in comparison of simulation and experiment.

separated until the end parts. In case of experimental and analysis results, the higher the height (h) of the beam, the greater the G CBT value.

4. Conclusions

As the experimental and simulation results of fracture behavior at DCB specimen of aluminum foam bonded with spray adhesive, the following conclusions are made:

(1) In case of experimental and analysis results, the higher the h, the height of the beam, the greater the maximum load. But the load is significantly reduced as displacement increases.

(2) In case of experimental and analysis results, the higher the height(h) of the beam, the greater the G CBT value. After the length of crack reached 150 mm, G CBT value in case of h = 40 mm is significantly reduced to the level below the data in case of h = 35 mm.

(3) Bending force is applied greatly just before the end part of crack and maximum stresses are shown at the end part of crack in cases of specimen heights of 25 mm, 30 mm and 35 mm. In cases of specimen height of 40 mm, maximum stress is shown at the end of bonded part. As crack propagates until the rear part of model in case of specimen height of 40 mm, the great stress happens at the rear part of model.

(4) The analysis result becomes similar to the behavior of real composite foam material. The trends due to specimen thicknesses are analyzed. This study result can suggest the basic data to design the structure of aluminum foam bonded using adhesive safely.

Acknowledgement

This research was supported by Basic Science Research Program through the National Research Foundation of Korea (NRF) funded by the Ministry of Education, Science and Technology (2011-0006548).

References

[1] U. H. Park, H. W. Lee, S. J. Kim, C. R. Lee and H. Kim, Stochastic characteristics of fatigue crack growth resistance of SM45C steel, *International journal of automotive technology*, 8 (5) (2007) 623-628.

[2] A. R. Shahani and M. Forqani, Static and dynamic fracture mechanics analysis of a DCB specimen considering shear deformation effects, *International Journal of Solids and Structures*, 41 (14) (2004) 3793-3807.

[3] H. Yoshihara and T. Kawamura, Mode I fracture toughness estimation of wood by DCB test. Composites Part A, *Applied Science and Manufacturing*, 37 (11) (2006) 2105-2113.

[4] M. M. Shokrieh, M. Heidari-Rarani and M. R. Ayatollahi, Interlaminar fracture toughness of unidirectional DCB specimens: A novel theoretical approach, *Polymer Testing*, 31 (1) (2012) 68-75.

[5] M. Khoshravan and F. A. Mehradadi, Fracture analysis in adhesive composite material/aluminum joints under mode-I loading; experimental and numerical approaches, *International Journal of Adhesion & Adhesives*, 39 (2012) 8-14.

[6] D. K. Park, A development of simple analysis model on bumper barrier impact and new IIHS bumper impact using the dynamically equivalent beam approach, *Journal of Mechanical Science and Technology*, 25 (12) (2011) 3107-3114.

[7] K. Y. Jeong, S. S. Cheon and M. B. Munshi, A constitutive model for polyurethane foam with strain rate sensitivity, *Journal of Mechanical Science and Technology*, 26 (7) (2012) 2033-2038.

[8] Q. Meng, F. Qu and S. Li, Experimental investigation on viscoplastic parameters of conditioned sands in earth pressure balance shield tunneling, *Journal of Mechanical Science and Technology*, 25 (9) (2011) 2259-2266.

[9] British standard, BS 7991. Determination of the Mode I Adhesive Fracture Energy G_{IC} of Structure Adhesives Using the Double Cantilever Beam (DBC) and Tapered Double Cantilever Beam (TDCB) Specimens, *Imperial College of Science and Technology (JISC)* (2001) 3-13.

[10] *International standards organization*, ISO 11343, Geneva (Switzerland) (1993).

[11] E. F. Rybicki and M. F. Kanninen, A finite element calculation of stress intensity factors by a modified crack closure integral, *Engineering Fracture Mechanics*, 9 (4) (1977) 753-976.

[12] J. U. Cho, A. Kinloch, B. Blackman, S. Rodriguez, C. D. Cho and S. K Lee, Fracture behaviour of adhesively-bonded composite materials under impact loading, *International Journal of Precision Engineering and Manufacturing*, 11 (1) (2010) 89-95.

Jae-Ung Cho received his M.S. and Doctor Degrees in Mechanical Engineering from Inha University, Incheon, Korea, in 1982 and 1986, respectively. Now he is a professor in Mechanical & Automotive Engineering of Kongju National University, Korea. He is interested in the areas of fracture mechanics(dynamic impact), composite material, fatigue and strength evaluation, and so on.